Hindawi Publishing Corporation
Journal of Nanomaterials
Volume 2016, Article ID 2103647, 5 pages
http://dx.doi.org/10.1155/2016/2103647

Research Article

Evaluation of NO Oxidation Properties over a Mn-Ce/γ-Al_2O_3 Catalyst

Pan Wang, Peng Luo, Junchen Yin, and Lili Lei

School of Automotive and Traffic Engineering, Jiangsu University, Zhenjiang 212013, China

Correspondence should be addressed to Pan Wang; wangpan@ujs.edu.cn

Received 3 March 2016; Accepted 12 April 2016

Academic Editor: Renyun Zhang

With the purpose of studying the effect of diesel oxidation catalyst (DOC) on the NO oxidation activity, a series of xMn10Ce/γ-Al_2O_3 ($x = 4, 6, 8$, and 10) catalysts were synthesized by acid-aided sol-gel method. The physicochemical properties of the catalysts were characterized by X-ray diffraction (XRD), scanning electron microscope (SEM), and Transmission Electron Microscope (TEM). Result showed that the crystalline size of MnO_x and CeO_2 ranges from 5 nm to 30 nm and manganese existed mainly in the catalysts in the form of manganese dioxide. Moreover, NO oxidation experiments were carried out to evaluate the activity of the catalysts; according to the results, 6Mn10Ce/γ-Al_2O_3 catalyst showed the supreme NO oxidation activity with a NO to NO_2 conversion rate of 83.5% at 300°C. Compared to 500 ppm NO inlet concentration, the NO conversion was higher than that of 750 and 1000 ppm NO over 6Mn10Ce/γ-Al_2O_3 catalyst in the temperature range of 150–300°C.

1. Introduction

Diesel engines are widely used as commercial vehicle power due to the higher thermal efficiency, durability, and fuel economy compared to gasoline engines. However, with increasingly stringent vehicle exhaust gas emission regulations and the attention to health, the NO_x (NO, NO_2) emission from diesel engines that caused many serious environmental problems, such as acid rain and photochemical smog, has met severe challenge [1, 2].

Recently, catalysis technique adopted to oxidize NO to NO_2 has been attracting enormous attention due to its role in several catalytic processes, such as NO_x reduced by SCR with hydrocarbons and soot combustion in the atmosphere of NO_x/O_2 [3, 4]. The diesel oxidation catalyst (DOC) can not only oxidize CO, HC, and PM, but also facilitate the oxidation of NO to NO_2, which is beneficial for NO_x removal by the downstream SCR or NSR units [5, 6]; for urea SCR, a NO_2 : NO ratio of 1 : 1 is the most effective. In the NSR process, NO needs to be oxidized to NO_2 before being absorbed by storage components during the lean phase. However, according to the literature [7], the amount of NO_2 in diesel engine exhaust is usually less than 10% in the total NO_x. Hence, to improve the NO_2/NO_x ration is of great necessity for the sake of improving the posttreatment efficiency.

Many metal mixed catalysts, such as CeO_2/ZrO_2 [8] and MnO_x-TiO_2 [9], can effectively oxidize NO to NO_2. The MnO_x-CeO_2 mixed oxides have been reported to have much higher catalytic activities compared to the individual CeO_2 and MnO_x, for the reason that the strong interaction between MnO_x and CeO_2 can form solid solution [10, 11]. Li and coworkers reported that Mn-Ce oxides were active for NO to NO_2 oxidation with about 80% NO conversion at 150°C over Mn-Co-Ce(20)-400 catalyst [12]. According to the literatures [13–16], CeO_2 has been widely studied for its oxygen storage and redox properties, among which the most important property is that ceria can store and release oxygen via the redox shift between Ce^{4+} and Ce^{3+} under oxidizing and reducing conditions.

In this work, in order to study the NO oxidation performance by DOC, Mn-Ce/γ-Al_2O_3 mixed oxides catalyst was synthesized by acid-aided sol-gel method. X-ray diffraction (XRD), scanning electron microscope (SEM), and Transmission Electron Microscope (TEM) were carried out to investigate the physicochemical properties of the catalyst structure, and NO oxidation experiments were carried out to evaluate the activities of the catalysts.

2. Experimental

2.1. Catalyst Preparation. A series of xMn10Ce/γ-Al_2O_3 (x = 4, 6, 8, and 10, wt%) catalysts were prepared by acid-aided sol-gel method as described in the literature [17]. First, $Ce(NO_3)_3 \cdot 6H_2O$, $C_4H_6MnO_4 \cdot 4H_2O$, and γ-Al_2O_3 were weighed by different Mn/Ce molar ratio and dissolved in deionized water, respectively, to obtain solution, into which citric acid was added, the amount of which was twice the sum of Ce^{3+} and Mn^{2+} total molar. Then polyethylene glycol, the quality of which is 10% of the citric acid, was introduced and magnet-stirred at 80°C until transparent gel was obtained. Then it was dried at 110°C for 24 h and calcined in air for 5 h at 500°C. Then the powder was ball-milled to obtain the required 20–40-mesh powder.

2.2. Catalyst Characterization. X-ray diffraction (XRD) of the as-prepared sample was measured on a Bruker D8 ADVANCE X-ray diffractometer with a Ni-filtered Cu Kα (λ = 0.154068 nm) radiation source at 40 kV and 40 mA. Powder XRD patterns were recorded at 0.02° interval in the range of $20^\circ \leq 2\theta \leq 80^\circ$ with a scanning velocity of 7° min^{-1}. The crystalline size was calculated by Scherrer's formula $D = K\lambda/(\beta \cos \theta)$. Transmission Electron Microscope (TEM) measurement was done by using a Philips Tecnai 12 microscope, with a 120 kV accelerating voltage. Before testing, the catalyst powder was ground and dispersed ultrasonically in anhydrous ethanol and then dropped onto a carbon-coated Cu grid of 200 mesh. Scanning electron microscope (SEM) testing was performed on JSM-7001F microscope made by JEOL. Accelerating voltage was 0.5–30 kV, magnification 10–800 K, and resolution 1.2 nm (30 kV)/3.0 nm (1 kV).

2.3. Catalyst Evaluation. The oxidation of NO to NO_2 activity was measured at the temperatures in the range of 150–450°C. The catalysts were placed in a fixed-bed quartz mircoreactor with an inside diameter of 10 mm and plugged and sandwiched between two silica wool layers to prevent the sample from being blown away. The gases used in the tests were 500 ppm NO, 10% O_2, and N_2 in balance with a total flow rate of 280 mL/min, giving a space velocity of 56,000 h^{-1}. The outlet NO and NO_2 concentrations were detected by Thermo Scientific Model 42i-HL NO_x Analyzer. Before each NO oxidation experiment, the catalyst sample was heated to 450°C in N_2 atmosphere for 30 min, in order to clean up the residual gases adsorbed in the catalyst surface, and then cooled to the required measurement temperatures.

3. Results and Discussion

3.1. XRD Characterization. The X-ray diffraction patterns of xMn10Ce/γ-Al_2O_3 (x = 4, 6, 8, and 10) catalysts are shown in Figure 1. As can be seen in Figure 1, all the samples exhibit characteristic peaks of γ-Al_2O_3 at 2θ = 25.74°, 35.32°, 37.93°, 43.53°, 53.72°, 57.65°, 66.68°, and 68.36° (JCPDS: PDF 10-0173). The main diffraction peaks at 2θ = 28.880°, 33.652°, 47.918°, and 56.762° were attributed to the (111), (200), (220), and (311) planes of cubic fluorite CeO_2 (JCPDS: PDF43-1002) [18, 19]. Moreover, the diffraction peaks of CeO_2 shifted to lower degrees for about 0.5°, the reason of which is that a part of Ce^{4+} ions is replaced by Mn^{4+} and Mn^{3+} to form solid solution [20]. According to Scherrer's formula, the crystalline size of CeO_2 (111) is 26 nm. Other two diffraction peaks at 2θ = 28.823° and 56.197° (which are overlapped with the peaks of CeO_2) are identified as the phase of MnO_2 (JCPDS: PDF 65-7467). In addition, when x = 4, the diffraction peaks of Mn_2O_3 are not detected by XRD, which is in accordance with the small amount of manganese oxides, while the intensity increased with x (when $x \geq 6$).

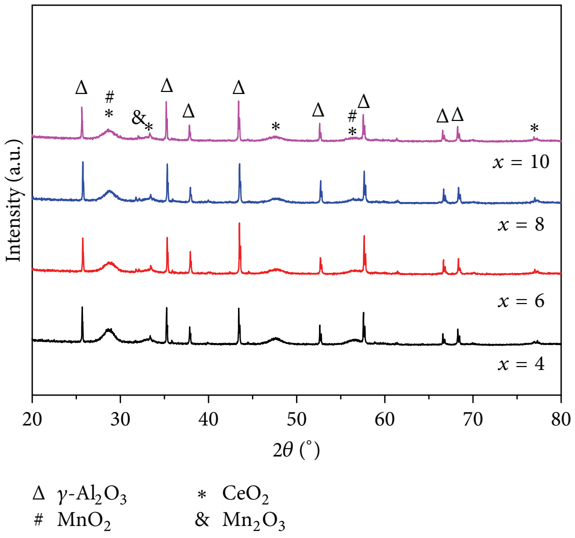

FIGURE 1: XRD pattern of xMn10Ce/γ-Al_2O_3 catalysts.

3.2. SEM and EDS Analysis. SEM analysis of as-prepared catalysts was used to elucidate the surface morphology and distribution of the different components present. Figure 2(a) shows the micrograph of 6Mn10Ce/γ-Al_2O_3 catalyst. As can be seen, the catalyst presents a morphology in the form of crisscrossed nanorods, which is γ-Al_2O_3, on which there are some particles of 10–30 nm (red circles) deposited that are CeO_2 nanoparticles; the result is in accordance with the XRD (the size of CeO_2 particle is 26 nm). In addition, some agglomerate particles with different sizes (80–300 nm) also deposited on γ-Al_2O_3, which can be the aggregates of MnO_x and CeO_2 (black circles). Figure 2(b) shows the surface elements of the sample; the main elements are Al, Mn, Ce, O, and C, which are from the white box area in Figure 2(a), among which the presence of C element can be attributed to the decomposition of citric acid and $C_4H_6MnO_4 \cdot 4H_2O$ at high temperature during calcination.

3.3. TEM Analysis. TEM is executed to ascertain the morphology of the catalyst. Figure 3 shows the morphology of 6Mn10Ce/γ-Al_2O_3 catalyst. Obviously, the main structure of

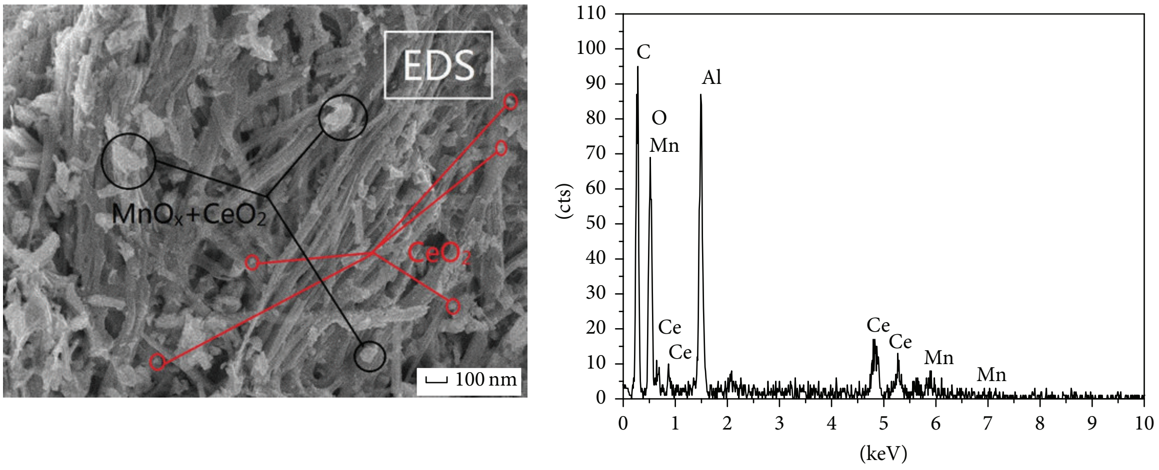

(a)

(b)

Figure 2: (a) SEM micrograph of 6Mn10Ce/γ-Al_2O_3 catalyst. (b) EDS pattern.

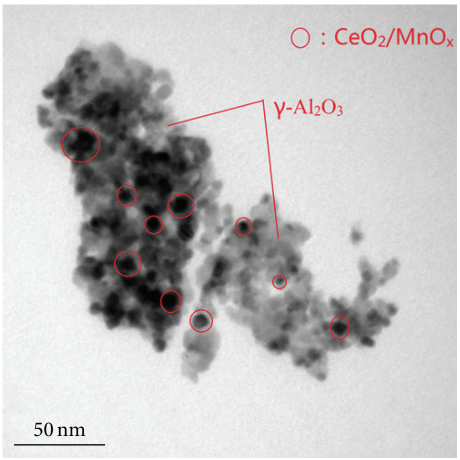

Figure 3: TEM pattern of 6Mn10Ce/γ-Al_2O_3 catalyst.

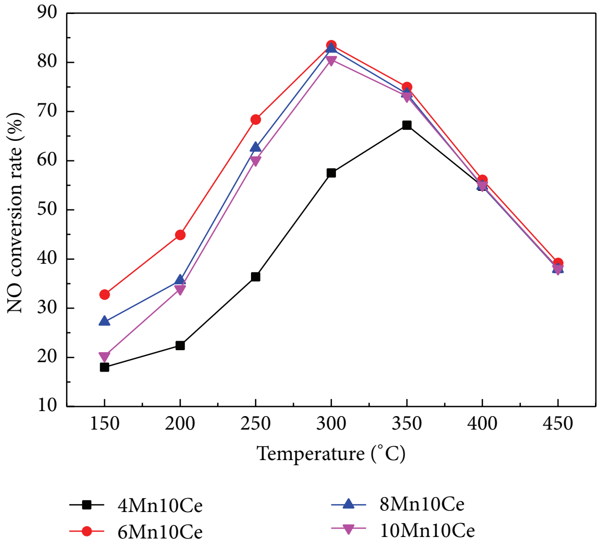

Figure 4: Oxidation activity of NO to NO_2 by O_2 on xMn10Ce/γ-Al_2O_3 ($x = 4$, 6, 8, and 10) catalysts at different temperatures (the conditions: 500 ppm NO, 10% O_2, N_2 in balance and 280 mL/min total flow rate, and space velocity 56,000 h^{-1}).

the catalyst is strip-shaped with nanosize, which is similar to the SEM analysis results. The small near-spherical particles with the size of about 5~30 nm (marked by the red circles), homogeneously dispersed on the surface of the catalyst, could be regarded as CeO_2 or MnO_x nanoparticles. Besides, the darker zone on the TEM pattern indicates a certain degree of aggregation between CeO_2 and MnO_x.

3.4. Effect of Temperature on NO Conversion. Results on NO conversion as a function of temperature over xMn10Ce/γ-Al_2O_3 (x = 4, 6, 8, and 10) catalysts are given in Figure 4. It is obvious that, in the range of 150°C to 300°C, NO conversion of all the catalysts increased with temperature, but when temperature is above 300°C, NO conversion decreased with temperature except for 4Mn10Ce/γ-Al_2O_3 catalyst (maximum NO conversion at 350°C). The NO conversion rate decreased mainly due to the accelerated thermal decomposition of NO_2 under the influence of high temperature. In the whole range of temperature, the steady-state NO conversion goes through a maximum of 83.5% at temperature of 300°C on 6Mn10Ce/γ-Al_2O_3 catalyst, followed by 8Mn10Ce/γ-Al_2O_3 (82.7% at 300°C), 10Mn10Ce/γ-Al_2O_3 (80.5% at 300°C), and 4Mn10Ce/γ-Al_2O_3 (67.2% at 350°C). Compared with other catalysts, 6Mn10Ce/γ-Al_2O_3 presented better NO oxidation activity. The reason was that the properties of the catalysts depend mainly on the active components, especially the Mn/Ce ratio. According to the research by Qi and Li [21], MnO_x are the main contributor for NO oxidation. Hence, with the increase of MnO_x, the catalysts showed better oxidation capacity, while the average chemical valence of Mn^{4+} decreased; the interaction between catalysts activities and Mn content is nonlinear. Therefore, in our research, the

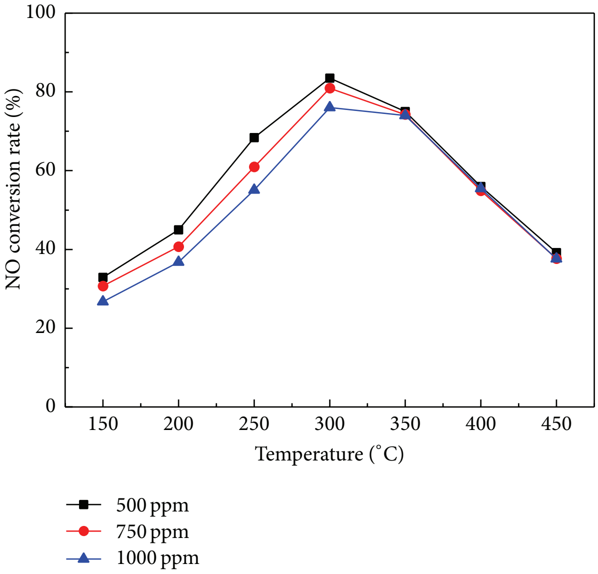

Figure 5: Oxidation activity of NO to NO_2 by O_2 on 6Mn10Ce/γ-Al_2O_3 catalyst at different temperatures (the conditions: 500, 750, and 1000 ppm NO, 10% O_2, N_2 in balance and 280 mL/min total flow rate, and space velocity 56,000 h^{-1}).

catalyst obtained the best NO oxidation activity when the Mn/Ce ratio is 6/10.

3.5. Effect of NO Concentration on NO Conversion. As described above, the 6Mn10Ce/γ-Al_2O_3 catalyst showed the best activity on NO to NO_2 conversion of 83.5% at 300°C. In order to further study the effect of inlet NO concentrations on the NO to NO_2 oxidation activity, the experiment, in the atmosphere of 500, 750, and 1000 ppm NO in 10% O_2 with N_2 as balance, respectively, was carried out. The NO conversion rate was calculated when the outlet NO concentration stabilized for 400 s. Results on NO conversion as a function of temperature over 6Mn10Ce/γ-Al_2O_3 catalyst are given in Figure 5. The result indicates that, in the range of 150–300°C, when inlet NO was 500 ppm, NO conversion rate was 32.9%–83.5%. In addition, with inlet NO concentration increasing, the NO conversion deceased by around 3% (NO = 750 ppm) and 5% (NO = 1000 ppm), respectively. Moreover, the NO conversion was almost maintained the same, whatever the inlet NO concentration in the range of 350–450°C was. However, the catalysts are sensitive to other pollution gases, such as SO_2, CO, and H_2O, which was still needed for further research.

4. Conclusions

In the present work, a series of xMn10Ce/γ-Al_2O_3 ($x = 4, 6, 8$, and 10) catalysts were prepared by acid-aided sol-gel method and found to be well crystallized and dispersed, CeO_2 and MnO_x with the crystalline size of 5–30 nm. Compared with other catalysts, 6Mn10Ce/γ-Al_2O_3 catalyst showed higher activity for NO oxidation to NO_2 over the temperature range of 150–450°C, up to 83.5% at 300°C.

In addition, NO oxidation to NO_2 was further studied under different NO concentrations over 6Mn10Ce/γ-Al_2O_3 catalyst. Generally, NO conversion augmented rapidly with temperature elevating in the range of 150–300°C for all different NO conditions. On the contrary, NO conversion decreased with temperature above 300°C. NO conversion reached maximum of 83.5%, 80.9%, and 76% for 500 ppm, 750 ppm, and 1000 ppm NO concentration, respectively, at 300°C. We also found that there was almost no effect of NO concentration on NO conversion above 350°C.

Competing Interests

The authors declare that there are no competing interests regarding the publication of this paper.

Acknowledgments

Financial support of this paper was provided by the National Natural Science Foundation (51206068), Natural Science Foundation of Jiangsu Province (BK2015040369), and State Key Laboratory of Engines, Tianjin University (K15-007).

References

[1] F. Cao, J. Xiang, S. Su, P. Wang, S. Hu, and L. Sun, "Ag modified Mn–Ce/γ-Al_2O_3 catalyst for selective catalytic reduction of NO with NH_3 at low-temperature," *Fuel Processing Technology*, vol. 135, pp. 66–72, 2015.

[2] V. Sanchez-Escribano, T. Montanari, and G. Busca, "Low temperature selective catalytic reduction of NOx by ammonia over H-ZSM-5: An IR study," *Applied Catalysis B: Environmental*, vol. 58, no. 1-2, pp. 19–23, 2005.

[3] C. Thomas, O. Gorce, F. Villain, and G. Djéga-Mariadassou, "Influence of the nature of the noble metal on the lean C_3H_6-assisted decomposition of NO on $Ce_{0.68}Zr_{0.32}O_2$-supported catalysts," *Journal of Molecular Catalysis A: Chemical*, vol. 249, no. 1-2, pp. 71–79, 2006.

[4] A. Russell and W. S. Epling, "Diesel oxidation catalysts," *Catalysis Reviews: Science and Engineering*, vol. 53, no. 4, pp. 337–423, 2011.

[5] I. Atribak, I. Such-Basanez, A. Bueno-Lopez et al., "Comparison of the catalytic activity of MO_2 (M=Ti, Zr, Ce) for soot oxidation under NO_x/O_2," *Achiv Fur Physikalische Therapie*, vol. 250, no. 1, pp. 75–84, 2007.

[6] J. Štěpánek, P. Kočí, F. Plát, M. Marek, and M. Kubíček, "Investigation of combined DOC and NSRC diesel car exhaust catalysts," *Computers and Chemical Engineering*, vol. 34, no. 5, pp. 744–752, 2010.

[7] G. Qi and W. Li, "NO oxidation to NO_2 over manganese-cerium mixed oxides," *Catalysis Today*, vol. 258, no. 1, pp. 205–213, 2015.

[8] Z. B. Wu, N. Tang, L. Xiao, Y. Liu, and H. Wang, "MnO_x/TiO_2 composite nanoxides synthesized by deposition-precipitation method as a superior catalyst for NO oxidation," *Journal of Colloid and Interface Science*, vol. 352, no. 1, pp. 143–148, 2010.

[9] I. Atribak, N. Guillén-Hurtado, A. Bueno-López, and A. García-García, "Influence of the physico-chemical properties of CeO_2-ZrO_2 mixed oxides on the catalytic oxidation of NO to NO_2," *Applied Surface Science*, vol. 256, no. 24, pp. 7706–7712, 2010.

[10] X. F. Tang, Y. G. Li, X. M. Huang et al., "MnO_x-CeO_2 mixed oxide catalysts for complete oxidation of formaldehyde: effect of preparation method and calcination temperature," *Applied Catalysis B: Environmental*, vol. 62, no. 3-4, pp. 265–273, 2006.

[11] H. Chen, A. Sayari, A. Adnot, and F. Larachi, "Composition-activity effects of Mn-Ce-O composites on phenol catalytic wet oxidation," *Applied Catalysis B: Environmental*, vol. 32, no. 3, pp. 195–204, 2001.

[12] K. Li, X. L. Tang, H. H. Yi, P. Ning, D. Kang, and C. Wang, "Low-temperature catalytic oxidation of NO over Mn–Co–Ce–Ox catalyst," *Chemical Engineering Journal*, vol. 192, pp. 99–104, 2012.

[13] S. F. Shi, Y. Q. Wang, J. C. Ma et al., "The preparation and performance of Ni–La/$Ce_xZr_{1-x}O_2$ catalysts for coupled methane partial oxidation/CH_4–CO_2 reforming to syngas," *Journal of Molecular Catalysis (China)*, vol. 27, no. 6, pp. 539–547, 2013.

[14] S.-J. Wang, G.-C. Zou, Y. Xu et al., "Ce-based catalysts for simultaneous removal of both diesel soot and NO_x," *Journal of Molecular Catalysis*, vol. 29, no. 1, pp. 60–67, 2015.

[15] L. W. Jia, M. Q. Shen, J. Wang, J. Wang, X. Chu, and W. Gu, "Durability of three-way and close-coupled catalysts for Euro IV regulation," *Journal of Rare Earths*, vol. 26, no. 6, pp. 827–830, 2008.

[16] H. Li, X. Tang, H. Yi, and L. Yu, "Low-temperature catalytic oxidation of NO over Mn-Ce-O_x catalyst," *Journal of Rare Earths*, vol. 28, no. 1, pp. 64–68, 2010.

[17] D. Delimaris and T. Ioannides, "VOC oxidation over MnO_x-CeO_2 catalysts prepared by a combustion method," *Applied Catalysis B: Environmental*, vol. 84, no. 1-2, pp. 303–312, 2008.

[18] C. Ming, D. Q. Ye, H. Liang, and H. Liu, "Catalytic combustion performance of soot over cerium-based transition metal composite oxide catalysts," *Acta Scientiae Circumstantiae*, vol. 30, no. 1, pp. 158–164, 2010.

[19] R. O. Fuentes and R. T. Baker, "Synthesis of nanocrystalline CeO_2–ZrO_2 solid solutions by a citrate complexation route: a thermochemical and structural study," *The Journal of Physical Chemistry C*, vol. 113, no. 3, pp. 914–924, 2009.

[20] Y. Rui, Y. Zhang, D. Liu et al., "A series of ceria supported lean-burn NO_x trap catalysts $LaCoO_3/K_2CO_3/CeO_2$ using perovskite as active component," *Chemical Engineering Journal*, vol. 260, pp. 357–367, 2015.

[21] G. S. Qi and W. Li, "NO oxidation to NO_2 over manganese-cerium mixed oxides," *Catalysis Today*, vol. 258, part 1, pp. 205–213, 2015.


Journal of
Nanotechnology


International Journal of
Corrosion


International Journal of
Polymer Science


Smart Materials
Research


Journal of
Composites


BioMed
Research International

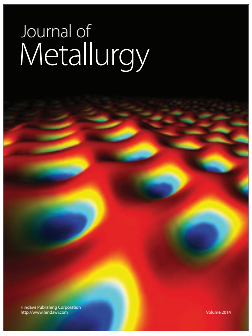
Journal of
Metallurgy


Journal of
Materials

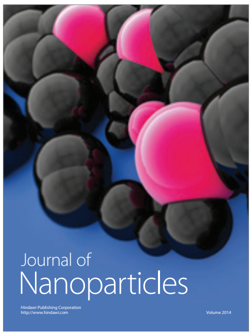
Journal of
Nanoparticles

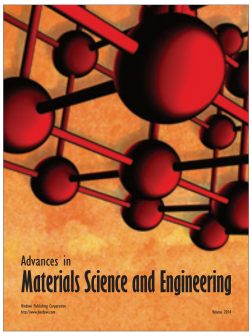
Advances in
Materials Science and Engineering

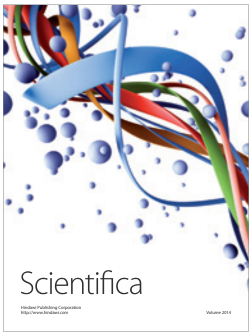
Scientifica

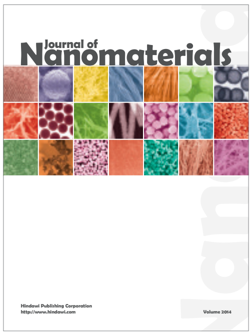
Journal of
Nanomaterials


The Scientific
World Journal


International Journal of
Biomaterials

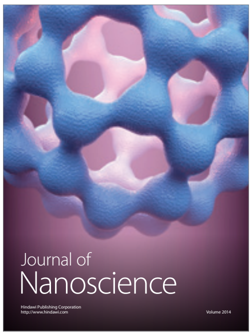
Journal of
Nanoscience


Journal of
Coatings

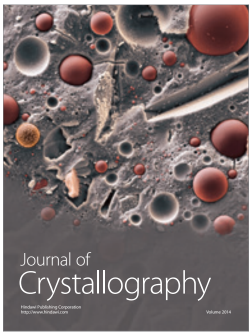
Journal of
Crystallography


Journal of
Ceramics


Journal of
Textiles